



HAL
open science

Evaluation of metallic bonded plates with nonlinear ultrasound and comparison with destructive testing

Paul Zabbal, Guillemette Ribay, Julien Jumel

► **To cite this version:**

Paul Zabbal, Guillemette Ribay, Julien Jumel. Evaluation of metallic bonded plates with nonlinear ultrasound and comparison with destructive testing. *NDT & E International*, 2021, 123, pp.102514. 10.1016/j.ndteint.2021.102514 . hal-03480641

HAL Id: hal-03480641

<https://hal.science/hal-03480641>

Submitted on 2 Aug 2023

HAL is a multi-disciplinary open access archive for the deposit and dissemination of scientific research documents, whether they are published or not. The documents may come from teaching and research institutions in France or abroad, or from public or private research centers.

L'archive ouverte pluridisciplinaire **HAL**, est destinée au dépôt et à la diffusion de documents scientifiques de niveau recherche, publiés ou non, émanant des établissements d'enseignement et de recherche français ou étrangers, des laboratoires publics ou privés.



Distributed under a Creative Commons Attribution - NonCommercial 4.0 International License

Evaluation of metallic bonded plates with nonlinear ultrasound and comparison with destructive testing

Paul Zabbal^{1*}, Guillemette Ribay^{1,2}, Julien Jumel^{2,3},

¹ CEA, LIST, Digiteo Labs, F-91191, Gif-sur-Yvette, France

²Univ. Bordeaux, CNRS, Bordeaux INP, Arts et métiers Paris Tech, I2M UMR 5295, F-33400 Talence, France

³Currently at Institut de Recherche Dupuy de Lome, 2 rue François Verny, 29200, Brest, France

*corresponding author, E-mail: Guillemette.ribay@cea.fr

Abstract

In the last decades, the use of structural adhesives has increased. Indeed, they are able to replace advantageously traditional assembly techniques such as riveting or bolting, and generally tend to reduce the global weight of the structure and/or improve the strength of the structure thanks to more homogeneous stress distribution. In addition, it allows the assembly of composite materials or materials having different nature, which is of great interest in the aeronautic industry. However, to be used for structural joining and critical application, reliable non-destructive testing techniques are compulsory for evident safety reasons, be it after fabrication or during the whole life of the structure. While linear ultrasounds have demonstrated their capability to detect easily decohesion or voids in a structure, their use for bond strength inspection is less straightforward. Another approach relies on the analysis of nonlinear signature of a bond defect inspected by high amplitude ultrasound. In the present paper, a Chaotic Cavity Transducer is used to inspect various metallic bonded plates (titanium or aluminum) with several bond defects. The defects were introduced by depositing localized surface pollution (introduction of PTFE spray, release agent, or fingerprints) before the adhesive is deposited on top of the surface. Combined with the pulse inversion technique, high amplitude plane waves were sent in the structure, leading to harmonic components observed in the defect region. Mechanical destructive tests were performed and display a good agreement with nondestructive tests.

Keywords: *Non Destructive Testing, nonlinear ultrasound, adhesion bond, Double Cantilever Beam test*

1. Introduction

Bonding is of great interest to replace traditional assembly techniques, as it makes it possible to lighten structures and/or improve their durability and strength through better stress distribution. However, the lack of robust non-destructive inspection

technique of bonding quality slows down its development, particularly in the aeronautic field. If the detection of severe defects such as delamination is easily done with classical ultrasound, the detection of weak bonds is less straightforward.

Probing interface weak bond by acoustic investigation techniques has been extensively studied for the last decades. Such methods include bulk ultrasound either in reflection (for instance [1], [2]) or through transmission (e.g. [3] [4]), linear guided waves such as Lamb waves (e.g. [5] [6]) or SH waves (e.g. [7]). The bonding quality is then determined using appropriate post-processing or inversion procedure based on the modelling of the bonded structure, in particular to distinguish the effect of bond thickness variation or bulk adhesive degradation from weak interfacial adhesion. For very thin trilayer structures (as the thinnest samples studied in this paper), adherend or adhesive thickness inhomogeneity makes it difficult to retrieve interfacial properties with these linear ultrasound methods [8] [9]. Non-contact, laser-based NDT methods were also shown to be able to distinguish a weak adhesion bond from a good one ([10] [11]). Another method using high power laser called Laser Shock Adhesion Test (LASAT) also proved able to detect weak bond in composite structures [12]. However, as explained by Ehrhart [13] a careful calibration must be done to limit the degradation by shock wave to the bondline.

In this paper, another approach is studied based on the nonlinear response of a weak adhesion bond subject to high amplitude ultrasound. The nonlinear response of an imperfect interface results from Contact Acoustic Nonlinearities activated by high amplitude ultrasound [14] and is less sensitive to bulk ultrasound properties or geometry of adhesive or adherends. The nonlinear response of an imperfect interface in a bonded structure has been studied in a laboratory environment for a couple decades [15] [16], In these papers, the imperfect interface between the adhesive and one adherend was created by applying a compressive load between two metallic planar blocks (one of whom with an adhesive layer), the defect being thus a kissing bond.

A more typical and dangerous bonding defect encountered in industrial environment is a weak bond induced by sparse contamination during bonding process. While the detection of a disbond due to a solid contamination layer (such as PTFE insert) is quite straightforward [17], a weak bond induced by lubricant spray, or induced by fingerprints after accidental touch by the operator, is more difficult to inspect. [12] and [13] were able to detect such contamination bonds in composite using laser shock waves (LASAT), but, as mentioned earlier, at the cost of the use of high power laser together with a careful calibration. Additionally, LASAT technique is destructive in the sense that weak interfaces are broken by the shock wave so that the remaining load carrying capacity of the interface is totally lost.

Unlike the aforementioned all-laser based techniques, the main objective of the present paper is to detect (and if possible characterize) weak bonding due to surface contamination using common laboratory low-cost equipment compatible with industrial constraints.. The second objective is to validate the method by comparison with quantitative mechanical destructive

tests, as it is rarely done in literature but strongly expected by industrials. As opposed to others contributions, specimens that are representative of industrial configurations are investigated. Also the NDE technique should be capable not only to detect the presence of weak bond but also to map the contour of the defect.

The present study focuses on the measurement of the second harmonic after high amplitude ultrasound emission by a Time Reversal Chaotic Cavity Transducer [18] [19]. Compared to Bou Matar's technique [19], in this work the Chaotic Cavity Transducer is not glued to the inspected sample to enable a unique calibration (see section 3.1), allowing the inspection of many samples without the need to repeat a time-consuming calibration procedure for each sample. Besides, unlike [19], its geometry is close to that of the Chaotic Cavity Transducer first introduced for medical application [20],

The procedure is applied to the nonlinear inspection of Aluminum or Titanium trilayer bonded samples representative of aeronautic structural bonds (thin adherends, thin adhesive layer, and industrial materials). The bonding procedure and introduction of intentional pollution is explained in Section 2. The Nonlinear Time Reversal Chaotic Cavity technique is described in section 3. Several DCB (Double Cantilever Beam) bonded specimens are subjected first to nonlinear ultrasonic inspection, and then to DCB mode I mechanical testing. Both experimental results are compared to validate the nonlinear nondestructive method and show whether it is effectively capable to localize weak bonded zones due to surface contamination.

2. Bonded samples preparation

Samples were prepared using aluminum (Al7075 T651) or Titanium (TA6V) adherends bonded with an epoxy film (AF191-U, manufactured by 3M [21]). Two types of Aluminum bonded specimen were prepared: one using 2mm-thick, 200mm wide and 200mm long adherends; and the other using 5mm thick aluminum adherend with other dimensions being compatible with Double Cantilever Beam (DCB) Test (following norm ASTM D3433), (viz. 200x25 mm²). These substrates are bonded with 100µm thick adhesive. Titanium samples are made with 1.6mm thick, 200mm long and 25mm wide adherends for DCB mechanical testing.

2.1. Bonding procedure

Surface preparation for Aluminum

The P2 chromium free [22] [23] surface preparation procedure (following ASTM E864) was applied to the aluminum adherend to achieve cohesive failure. Firstly, adherends are degreased to remove organic and polluting substance in an acetone ultrasonic bath at 30°C for 10 minutes. Then they are rinsed and immersed in a sodium hydroxide solution for 10 minutes at 40°C. A

black oxide superficial layer appears. Lastly, after being rinsed, they are put in a nitric acid bath to remove the oxide layer, before being rinsed again and dried with hot air.

A second etching is then applied to the substrates using a sulfuric acid/ferric sulfate III bath (called 'P2' [22]) at 65°C for 10 minutes. As a result, the external surface presents a specific texture enabling a good mechanical bonding. Figure 1 on the left shows how a deionized water droplet dropped on the surface is totally spread (wettability test). In the following section, the effect of surface pollution on the droplet spreading will be shown.

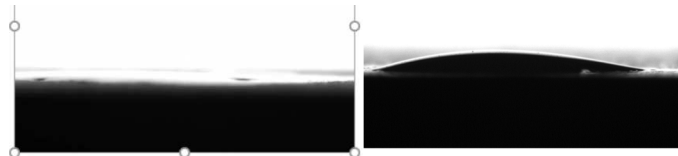


Figure 1 : Left: sessile wetting test of a nominally prepared surface. The drop is wholly spread on the metallic surface. Right: same test on a substrate nominally prepared then polluted with release agent spray.

Surface preparation for Titanium

Titanium substrates were prepared by Protec company following an industrial confidential process including etching, then conversion stage. An adhesion promoter is also applied to achieve appropriate bonding performance for a minimum of 6 months.

Bonding and curing (for both aluminum and titanium)

After surface preparation, Af191-U non-supported film adhesive is applied immediately to avoid any kind of unwanted pollution. A PTFE glass cloth adhesive mask is placed on top of one adherend to control the bond-line thickness and bonded area. Moreover, it serves as initial crack length in DCB tests (see section 4.1). The two adherends are placed in an alignment jig then pressed together with a press to remove possible entrapped air. Curing is done in a vacuum bag placed in an autoclave at 180°C and 4 bar pressure for one hour. The pressure in the vacuum bag is maintained at 300mbar during curing.

2.2. Introduction of defects

Reference bonded specimens are produced following the above-mentioned procedure. Samples with controlled bonding degradation are obtained by introducing pollution on top of one adherend surface right after surface preparation. Three types of pollution are tested: a spray of release agent (SANSIL SF 772), a spray of PTFE (PTFE Dry Film Lube RS™), and a fingerprint. Figure 1 (on the right) and Figure 2 (on the left and on the right) evidence the increase of contact angle during

sessile drop wetting test due to surface pollution. While with the P2 surface preparation procedure the droplet is almost totally spread on the adherend surface (see Figure 1 on the left), c.a. 10° contact angle is found with the release agent pollution (see Figure 1 on the right). As shown in Figure 2, c.a. 90° and 70° are also found respectively for the PTFE spray (Figure 2 on the left) and the finger print (Figure 2 on the right). Consequently, reduced mechanical performance of the bonded interface should be observed on the specimens containing such pollutions since poor wetting of adhesive, and surface pollution generally produces weak bond or even kissing bond. However, detrimental effect of the pollution introduced here should be assessed by mechanical characterization tests as described in section 4.

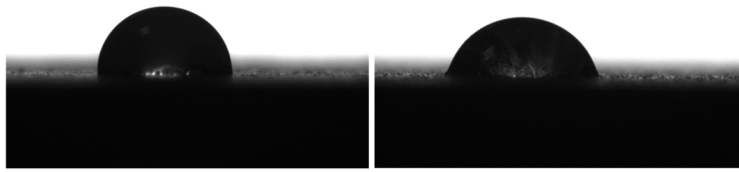


Figure 2: Left: Sessile wetting test of a substrate nominally prepared then polluted with PTFE spray. Right: same test on a substrate nominally prepared then polluted with a fingerprint.

3. Non-linear inspection method

3.1 Time Reversal Chaotic cavity transducer

The bonded specimens are inspected using high amplitude ultrasonic waves to activate potential contact nonlinearities in the vicinity of an imperfect interface.

As shown by Quieffin [20], and Montaldo [18] for medical imaging, Time Reversal (TR) of ultrasound in a reverberant metallic bloc allows ultrasonic energy to be focused both in time and space. If the metallic bloc has an ergodic shape, TR focusing is possible at any point of the bloc that is then called a Chaotic Cavity. Provided the cavity is reverberant enough (depending on the intrinsic attenuation of the cavity and boundary conditions), TR focusing is obtained with a single ultrasound transducer glued on the cavity. This has also been proved useful in Non Destructive Testing, where the cavity (with one or several classic ultrasonic transducers glued on it) is used as a whole transducer and is called the Chaotic Cavity Transducer [19] [24] [25].

Before using the Chaotic Cavity Transducer for NDT, a calibration procedure (see Figure 3) is performed (corresponding to the learning phase or forward propagation phase of any Time Reversal Process). It consists in learning all impulse responses between each transducer glued on the cavity and each point (red dots in Figure 3) at the surface of the cavity where one wants to focus ultrasound. This is usually done using non-contact measurement like

laser interferometer.

Typical impulse responses in a reverberant cavity are very long, coda-like signals; the longer the reverberated signals, the higher their energy content.

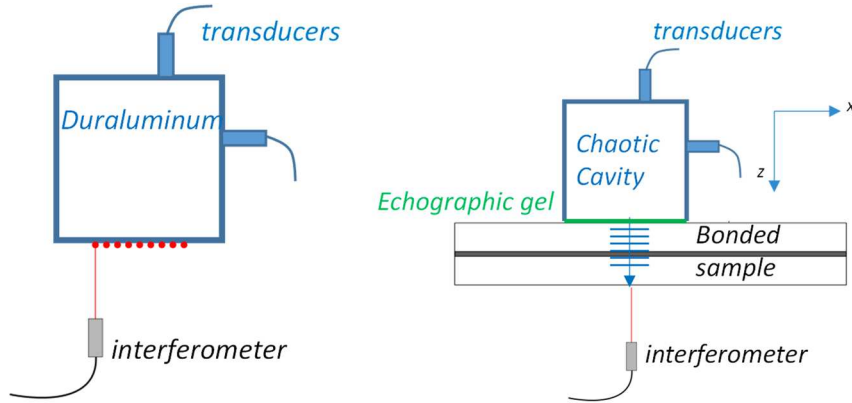


Figure 3: Steps of a Time Reversal Experiment. Left, calibration procedure: learning of impulse responses between transducers glued on the chaotic cavity and several red dots on the bottom surface using a laser interferometer. Right, through transmission inspection of a bonded sample with high amplitude plane wave: backpropagation after appropriate time reversal and combination of impulse responses. *(color should be used in print)*

Let us consider one impulse response (IR) between one ultrasonic transducer and one given desired focusing point A. If this IR was reversed in time and reemitted by the same transducer (which is called the backpropagation phase), thanks to the invariance of wave propagation equations with time reversal and spatial reciprocity [26], the energy would focus back in time at point A in the form of a high amplitude pulse, with the same energy content as the IR. The minimum spatial width of the focusing point is theoretically equal to half the wavelength of bulk wave in the cavity [26] [20].

Even though focusing after TR is supposed to occur when the boundary conditions are the same in the learning phase as in the backpropagation phase, TR has been shown to be robust to some changes, for instance the immersion in water in the focusing step (whereas the cavity is surrounded by air in the learning phase [20]). However, previous research using a chaotic cavity transducer for NDT did not make use of this property. Indeed, the cavity was glued on the component [19], [24], [25] the learning phase was thus performed directly on the component. Consequently, the coda-like signal measured in the learning phase contained both reverberated signals in the cavity and reverberated signals in the component. For each new component to inspect, the learning phase needed thus to be repeated.

In this paper, however, to avoid a too strong breach of symmetry between calibration (=learning phase) and use in an

inspection (=backpropagation) phase, ultrasonic coupling gel (whose ultrasonic impedance is close to that of water) is placed between the cavity and the sample (see figure 6). The following experiments will demonstrate whether this breach of symmetry is indeed small enough to ensure a proper focusing after Time Reversal with the Chaotic Cavity.

3.2 Application of the Chaotic Cavity Transducer to nonlinear NDT of bonded samples

The chaotic cavity geometry chosen in our study is based on Montaldo's work in medical imaging [18] as it allows a chaotic reverberation of waves in 3D (see Figure 4). It is a 50 mm x 50mm x50mm piece of Duraluminum with a spheric hole. Unlike previous use of Chaotic cavity in NDT [19], such a 3D geometry is necessary here to allow an homogeneous focused amplitude at any chosen point of the output surface (surface in contact with the bonded structure), as already proven by [20].

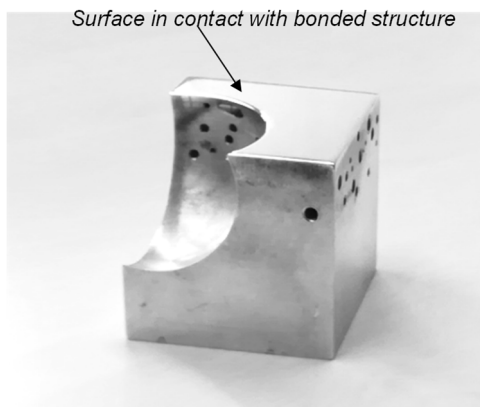


Figure 4: Chaotic Cavity used in the experiments

The ultrasonic transducer frequency is 500kHz, which was a good compromise between too wide focusing spot and too high attenuation in the cavity (as ultrasonic attenuation of bulk waves increases with frequency [27]). Two 12.7mm diameter Sofranel transducers (PSLM 50.5, central frequency 500kHz) are glued on the cavity (Figure 3 on the right). All electric signals fed into the transducers are maximum 70Vpp (as in classical linear NDT) to avoid any nonlinear effect in the electronic system and in the cavity itself.

Impulse responses are measured during the calibration procedure (learning phase) using coded signals called Maximum Length Sequence (MLS). MLS is a classic method of measuring IR in Room Acoustics [28] [29]. Among many studies about the best method of measuring impulse response in a linear system (for instance [30], [31]), MLS is preferred when the system nonlinearity is negligible, and is particularly immune to noise. MLS generated by Python software are used in this study. The signal measured by the laser interferometer in the calibration procedure is then

equal to the IR convolved with the coded signal. Using the auto-correlation property of MLS and the linearity of the system, the IR are then computed. IR are then time-reversed, converted into 1-bit signals (+1 if the amplitude is positive, -1 if it is negative), and lastly low pass filtered using a butterworth filter with cutoff frequency 700kHz. The signal was filtered after doing the 1-bit operation because such an operation generates a signal with a large frequency bandwidth, including frequencies we do not want to be transmitted (even with very low amplitude) by the transducer, namely around 1MHz, as they could prevent us from measuring properly the second-harmonic response of a potential weak bond.

This procedure is illustrated in Figure 5. Before 1bit processing, the impulse response is cut to suppress the coda when its amplitude is lower than twice the noise level (the latter is measured before the start of the impulse response), as shown by the selected zone (arrow in Figure 5.c).

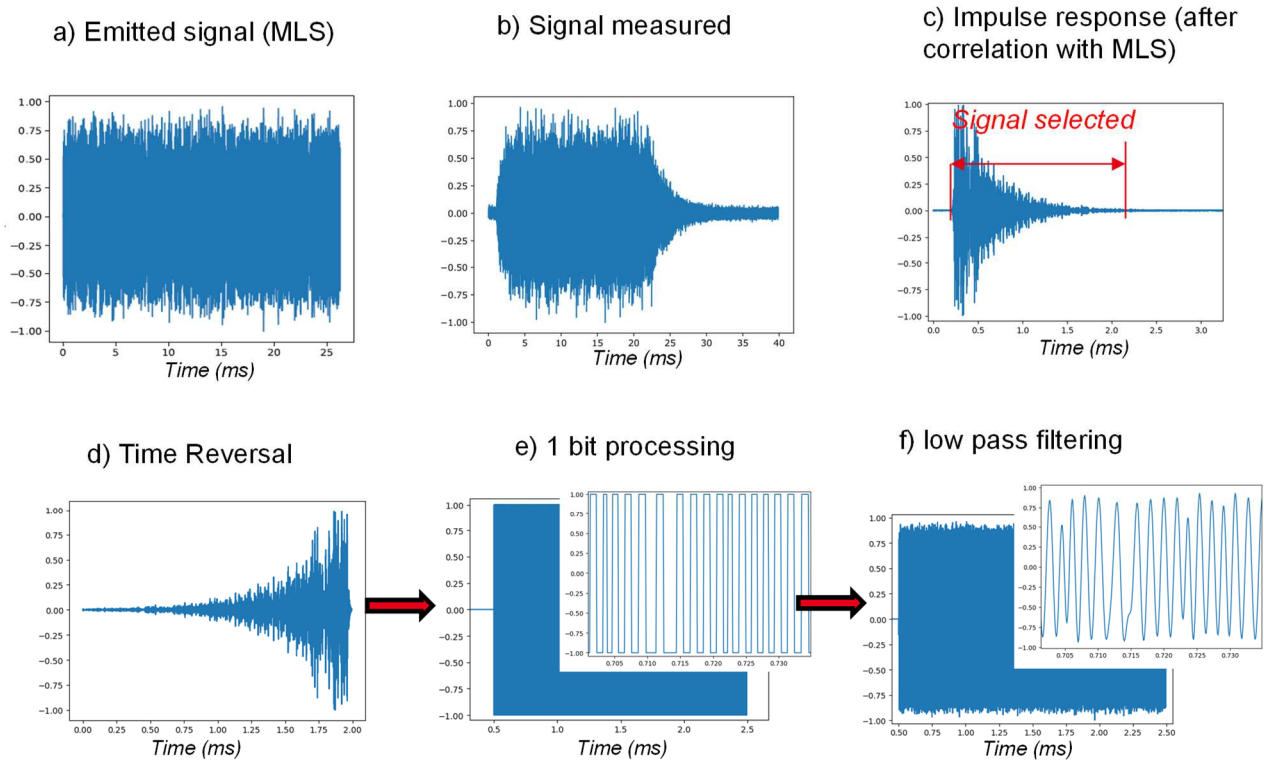


Figure 5: Processing steps of the signal measured at one point on the cavity, after transmission of a MLS (a). After measurement (b), the signal is correlated with the emitted MLS to retrieve the impulse response (c). The signal is cut (see arrow in c), then time-reversed (d), converted to 1bit (e), and lastly low-pass filtered (f).

The Chaotic Cavity Transducer can then be used for NDT as a simple transducer, and placed anywhere needed on the bonded structure. A 2-channels arbitrary waveform generator (Keysight™ 33500B) connected to a linear amplifier (NFT™ HSA 4101) is used to feed both ultrasonic transducers glued on the cavity with the filtered time-reversed

impulse response, scaled to maximum 70V_{pp}.

Moreover, linearity of wave propagation in the cavity allows us to linearly combine impulse responses between both transducers and any desired focusing point on the cavity surface in contact with the inspected sample. Therefore, impulse responses between every point on a 10mm square grid with a 1mm step and each transducer glued on the cavity are measured and processed as illustrated in Figure 5. For each transducer, the processed IR are combined so that after back-propagation, ultrasonic waves focus simultaneously on all points of the grid. The resulting wavefield takes the form of a locally plane wave with a half-width amplitude of 6.3mm. The procedure was described in a previous paper by the authors [9].

The experimental set-up used for bonded samples inspection is the same as in [9] and is presented in Figure 3. A laser interferometer (Polytec OFV534) is used in transmission to collect the ultrasonic wave after propagation through the bond-line. The laser interferometer could easily be replaced with a simple contact transducer with a central frequency 1MHz to collect the second harmonic component. However, we chose here to use the interferometer as its large bandwidth allows collecting simultaneously the fundamental frequency and all potential harmonics and gives an absolute measurement of the out-of-plane displacement in nm for easy comparison with literature. Moreover, laser interferometer measurement directly at the Chaotic Cavity output surface after backpropagation proved that no harmonic component is indeed emitted by the cavity (harmonic amplitude is 60dB below the maximum at the fundamental frequency).

The peak-focused amplitude measured on the opposite surface of a nominal bonded Aluminum sample with the laser interferometer is 12nm.

3.3 Nonlinear measurement with pulse inversion

The nonlinear inspection bonded planar procedure is illustrated in Figure 6 and Figure 7. The inspection is performed twice, once with the regular IR, the second with the opposite of the IR to create an opposite pulse after TR focusing. This process, called pulse inversion [32] is classically used in nonlinear medical imaging to reduce the fundamental component and enhance the harmonics created by interaction of the fundamental wave with nonlinearity (eg

microbubbles). The relatively weak voltage applied to the ultrasonic transducers glued on the cavity allows us to use this process, without damaging the piezo-electric disk. Given that the harmonic components created by CAN are several order of magnitude lower than the fundamental incident component, the Signal to Noise Ratio is weak and pulse inversion is a very efficient way to enhance it [33].

Both transmitted waves are then summed, as illustrated in Figure 6 after transmission through a PTFE polluted Aluminum sample. The amplitude of the second harmonic component is then measured after computation of DFT in Python software. The harmonic amplitude is expressed in percentage of the amplitude at the fundamental frequency (measured before pulse inversion), see Figure 7. Note that the fundamental component is not completely suppressed here.

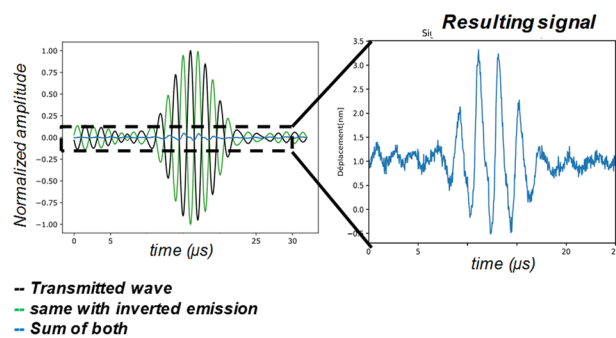


Figure 6: Example of wave measured by interferometer after propagation through an imperfect bonded sample: use of pulse inversion to enhance non-linear signature of an interfacial defect. *(color should be used in print)*

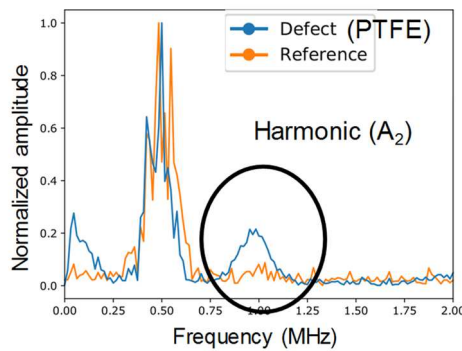


Figure 7: Typical amplitude spectrum of the resulting signal, measured on a Al-AF191-Al perfect bonded sample ('reference', orange line) and bond where PTFE spray was applied to one adherend prior to bonding (blue line). *(color should be used in print)*

To illustrate the procedure, the measurement was done first on a nominally bonded Aluminum sample, then on a PTFE

polluted bonded Aluminum sample, with increasing voltage applied to the transducers glued to the cavity. As presented in Figure 8, the percentage of the second harmonic increases with the excitation voltage only when inspecting the degraded bonded sample, and stays below 6% when inspecting the nominally bonded sample. The degraded bond thus displays a nonlinear ultrasonic response.

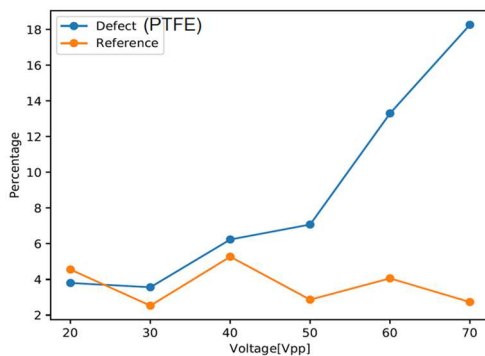


Figure 8: Amplitude of second harmonic (in percentage of amplitude at fundamental frequency) versus voltage applied to emitters, for defect-free aluminum bonded sample (orange line) and defect aluminum bonded sample (PTFE applied to one substrate prior to bonding). (*color should be used in print*)

The objective of the following section is to check whether a nonlinear signature can be measured on several bonded samples with different pollutions applied on one adherend prior to bonding, and whether it is indeed correlated with a reduction in bond strength.

4. Comparison of nonlinear inspection with destructive tests

4.1. Double cantilever beam (DCB) testing

Among many possible destructive mechanical tests described in the literature to characterize bonded interfaces (peel, single lap shear, butt joint...) [34] [35], the Double Cantilever Beam is used here (following norm ASTM D 3433). It allows the calculation of the interface Critical Strain Energy Release Rate which characterize the capacity of the bonded to resist to a quasi-static crack propagation [36]. It has been previously used to evaluate the effect of surface contamination in bonded specimens [37]. Compared to other tests configuration, the specimen geometry allows the manufacturing of large bonded area and thus application on a same specimen of proper surface preparation and surface pollution. This geometry is applicable for thick or thin adherends.

The specimen consists in two flexible bonded slabs, a large PTFE insert being places on one end of the bondline mimicking an initial crack. Each adherend of the specimen is attached on the pre-cracked edge to a dual actuator system composed of two EZ001 Zwick electromechanical actuators (maximum force 1kN); see Figure 9. A constant opening displacement rate is

applied to the actuator system (1mm/s) in a symmetrical configuration to initiate and propagate the bondline decohesion. The force P applied to maintain this opening rate is recorded during the whole process.

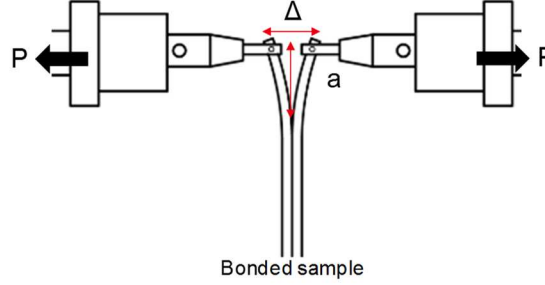


Figure 9: DCB test: opening force applied with constant opening rate. a is the effective crack length, and Δ the opening displacement.

The theoretical force-displacement curve during DCB test considering brittle interface and elastically deforming adherend are determined using linear fracture mechanics concepts [38]. Two regimes are expected: first a reversible elastic loading phase where no fracture appears in the sample (on the left), then a crack propagation regime where the force P decreases as the crack propagates. The specimen strain energy release rate (SERR) for a DCB test is given by relation:

$$G = \frac{a_{eff}^2 P^2}{wEI} \quad (1)$$

with E being the adherend Young's modulus, $I = wt^3/12$, the second moment of inertia of the adherend cross section (t is the adherend thickness, w the width of the adherend). For proper evaluation of the SERR, various crack length correction methods could be used to take into account interface compliances, and other experimental artefact. Here, the effective crack length technique is used [37], [39] where the effective crack length a_{eff} is determined from the specimen compliance value (defined as Δ/P),

$$\frac{\Delta}{P} = \frac{2a_{eff}^3}{3EI} \quad (2)$$

The crack propagates when the condition $G = G_c$, is reached G_c being the critical SERR. Assuming a uniform bondline, G_c can be considered to be constant along the crack propagation path. Then combining relation (1) and (2), with the condition $G = G_c$, the force versus opening displacement evolution during the crack propagation regime is determined.

4.2. Checking of repeatability of bonding

Two aluminum bonded joints prepared using the P2 surface etching procedure are tested first. The force-displacement curves (Figure 10) and measured SERR (Figure 11) are almost identical for both specimens. Moreover, their fracture surfaces (Figure 12) reveal cohesive failure (glue is seen on both adherends after breaking, the crack is propagating along the middle of the bondline), as required for industrial process qualification. Unlike the theoretical curve, the measured force-displacement exhibit stick-slip behavior which is due mainly to viscous behavior of the adhesive (see whiter lines in Figure 12) [40]. The critical SERR G_c is then computed as the mean of G values measured at onset of each dynamic crack propagation step (Figure 11). The observation of the fracture surfaces shows that each propagation start and arrest positions are the same for both adherends which confirms that this phenomenon is due to the sole joint behavior but not to the presence of defect or bondline variability.

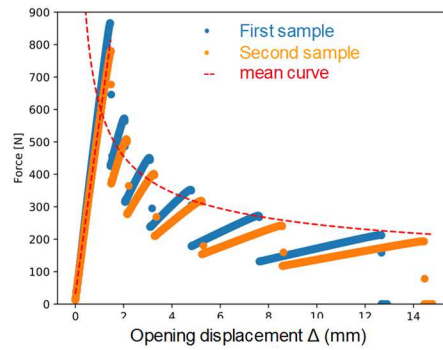


Figure 10: Experimental force-displacement curve measured on two identically manufactured bonded AL-AF191-AL samples with nominal procedure. – mean curve theoretical $P(\Delta)$ evolution assuming constant G_c . *(color should be used in print)*

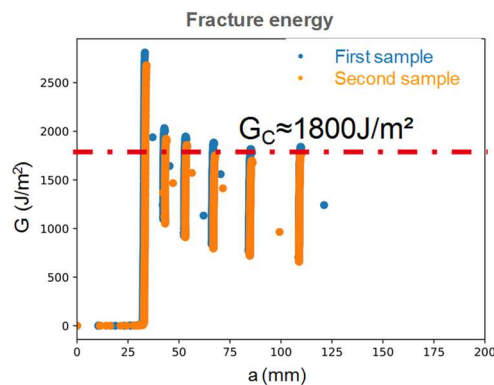


Figure 11: Experimental strain energy release rate (SERR) as a function of crack length inferred from the force-displacement curve measured for two perfectly bonded Al-AF191-Al samples. *(color should be used in print)*

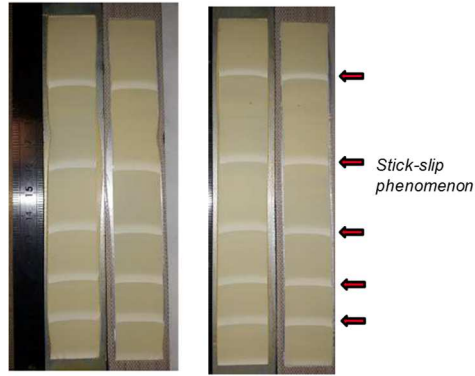


Figure 12: Fracture surfaces observed after DCB test on the same Al-AF191-Al nominally bonded samples used in figures 7 and 8. (*color should be used in print*)

4.3. Inspection of Al-AF191-Al bonded samples with various pollutions

4.3.1. 2D scanning of non-linear parameter on aluminum thin bonded samples

Additional specimens were manufactured as described in section 2.1 and subjected to nonlinear NDT prior to DCB mechanical testing. The nonlinear through transmission inspection procedure is repeated for several chaotic cavity/laser interferometer positions (both moving together to ensure the laser beam stays aligned with the middle of the active emitting surface of the cavity), both along the length and width of the sample. All nonlinear experiments are performed with a maximum peak-to-peak amplitude of 70V applied to both transducers glued to the cavity. At each position, the second harmonic is measured (after pulse inversion) and expressed as a percentage of the fundamental component amplitude (before pulse inversion).

First, two 2mm Aluminum/0.1mm AF191/2mm Aluminum specimen are manufactured, one with nominal bonding procedure, the other with uniform PTFE sprayed on one adherend before bonding. They are inspected every mm on a 100mm by 15mm region with the nonlinear inspection system. Figure 13 shows the map of harmonic percentage for a nominally bonded aluminum sample (on the left) and a PTFE polluted bonded aluminum sample (on the right). The mean value measured on the PTFE polluted sample is 12.7% (3.4% standard deviation) whereas it is 3.8% (1.3% standard deviation) on the perfectly bonded sample. A good bond seems thus to be distinguished from a degraded bond.

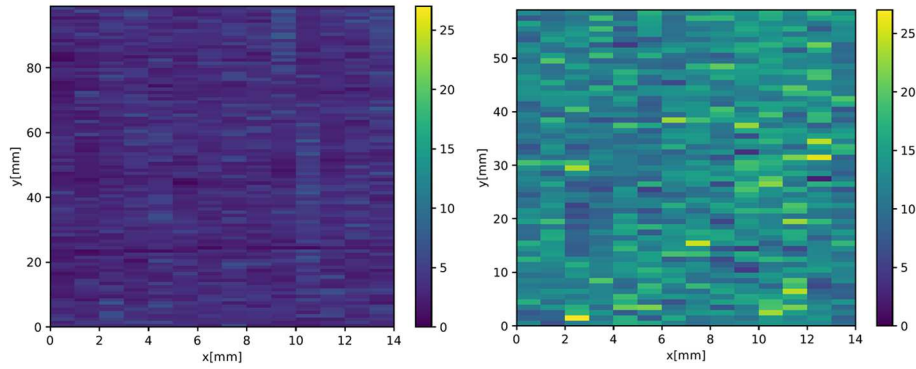


Figure 13: Second harmonic amplitude (percentage of fundamental component) measured on two bonded Al-AF191-Al samples, with nominal bonding (left) and pollution with PTFE spray (right). (*color should be used in print*)

A second Aluminum sample with two fingerprints representative of operator mishandling of adherends before bonding was inspected with the chaotic cavity. As shown in Figure 14, the second harmonic level increases in the region of the fingerprint. Note that in this case the second harmonic level is expressed in a logarithmic scale as the defect was more difficult to observe in a linear scale. The method seems thus able to detect such a weak defect.

When the method is applied to inspect samples made of the same material (adherends and adhesive) with the same thicknesses and geometry, using the same amplitude of incident wave, the second harmonic level could be used as an absolute measurement, thus allowing comparison between samples; Figure 13 shows that this is possible for PTFE spray contamination defects. However, a uniform pollution of the whole bond of a given structure is unlikely to occur in practice; in most cases, a relative comparison between well-bonded part and defect area of the bonded structure would be enough to detect a defective bond. In that case, fingerprints can be detected by the method.

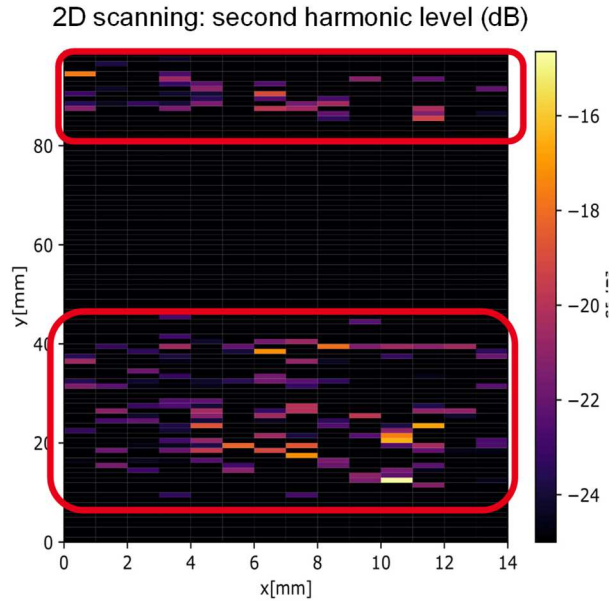


Figure 14: Second harmonic amplitude (divided by fundamental amplitude and expressed in dB) measured on an Aluminum bonded sample with pollution with fingerprints right after surface preparation. The actual positions of fingerprints are circled in red. (*color should be used in print*)

4.3.2. Inspection of a bonded specimen with localized pollution and comparison with mechanical DCB test

The thin Aluminum specimen geometry used in the previous experiments is representative of thin bonded structures used in aerospace industry, but is not suited for DCB destructive tests (as the aluminum would undergo plastic deformation before propagation of crack). Further experiments were thus performed on thicker (and smaller in width) bonded Aluminum specimen to compare nonlinear NDT with DCB characterization.

A bonded specimen was prepared containing PTFE pollution on one-half of one adherend right after surface preparation (Figure 15 on the left). The other side is left clean by masking the area during spraying. After DCB test, the fracture surfaces display a cohesive failure along the clean region, and an adhesive failure along the polluted region as revealed by the metallic aspect of the fractured surface. After destructive test is performed, local observations are performed using a Scanning Electron Microscope to observe the transition between cohesive and adhesive failure which are shown in Figure 16. From the secondary electron observation, a step is revealed indicating that the crack front moved from the middle of the bondline to a position close to the surface polluted by the PTFE spray. With the backscatter electron observation, a clear separation between adhesive and cohesive failure region is observed again. The PTFE particle clearly prevent the adhesive from properly adhering to the aluminum surface as revealed by the white spots where almost no adhesive is detected.

Nonlinear ultrasound NDT was performed on a rectangular zone (see dash line in Figure 15 on the left) covering partly both the polluted and perfectly bonded regions.

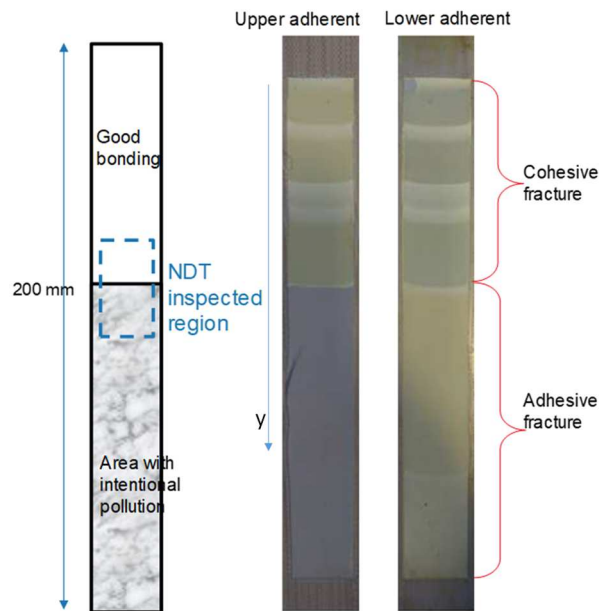


Figure 15: Al-AF191-Al sample with PTFE pollution on a half (sketch on the left, and fracture surfaces after DCB test on the right). The crack front moved from good bonding region to polluted region (along y axis). The region inspected with non-linear US is highlighted in a dashed blue line. *(color should be used in print)*

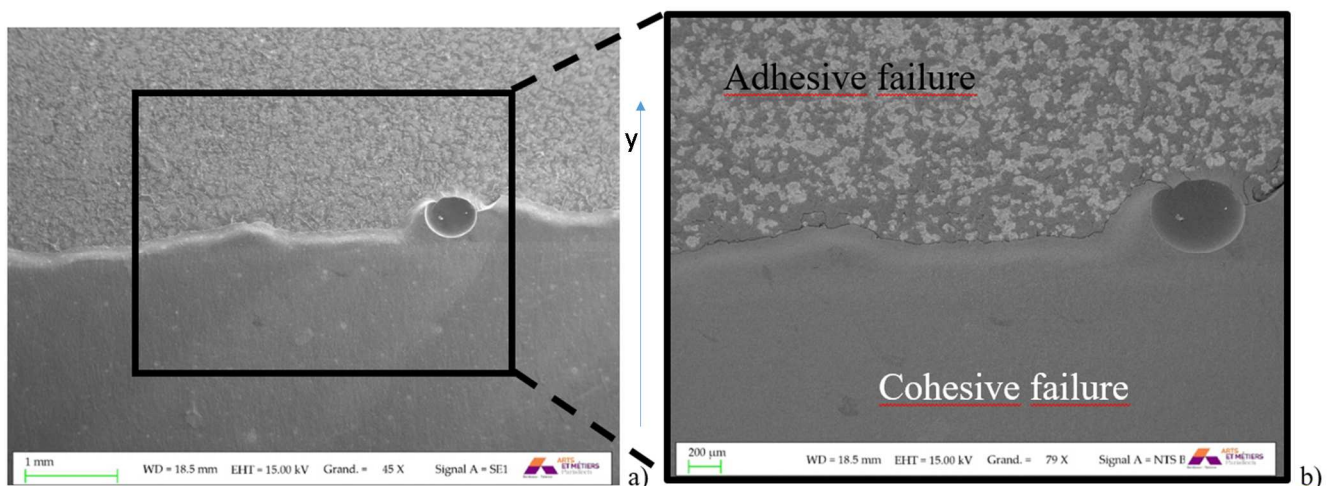


Figure 16.a) secondary electron, b) backscattered electron observations of the transition line between cohesive and adhesive fracture surface of upper adherend shown in Figure 15

The second harmonic level (in percentage of the fundamental component) is represented in Figure 17. It increases in the polluted region.

DCB force-displacement curve and Strain Energy Release Rate (SERR) measured on a nominally bonded aluminum sample and the half-polluted PTFE sample are shown in Figure 18. On the first half (with no pollution), both samples curves are almost identical ; when the crack reaches the PTFE region, the force needed to open it is significantly lower than for the nominal bonded sample. The same conclusion can be drawn from the SERR measurement. The DCB test is thus in good agreement with the nonlinear ultrasound NDT measurement.

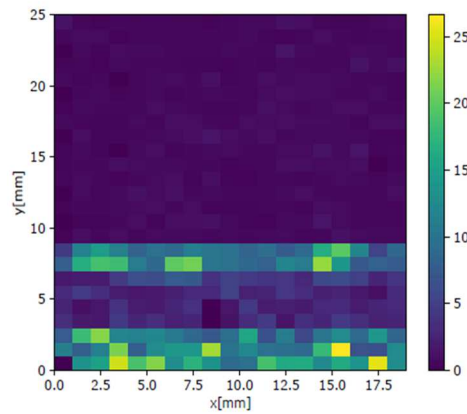


Figure 17: Second harmonic amplitude (percentage of fundamental amplitude) measurement on Aluminum bonded sample with PTFE sprayed on a half of one substrate before bonding. *(color should be used in print)*

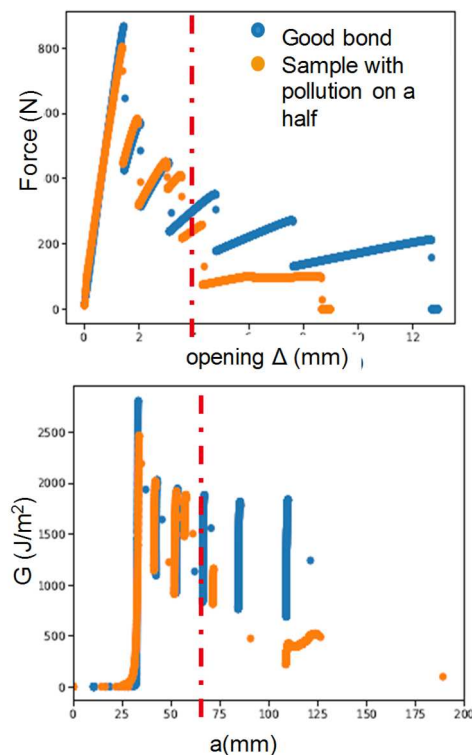


Figure 18: Force-displacement curve (on top) measured via DCB test on the Aluminum bonded sample with PTFE on one-half (orange dots) versus nominally bonded sample (blue dots); resulting SERR for both cases (bottom). (*color should be used in print*)

4.4. Inspection of Ti-AF191-Ti bonded samples

DCB 1.6mm/0.1mm/1.6mm Titanium/AF191/Titanium bonded specimen are then manufactured, either with nominal bonding procedure or with uniform release agent spray pollution or PTFE spray pollution on one adherend prior to bonding. Both nonlinear inspection and DCB testing are performed. Fracture surfaces (Figure 19) reveal cohesive failure for the nominal bonded sample and adhesive failure (presence of adhesive on only one adherend) for both PTFE and release agent polluted samples, as a sign of degraded bond strength. DCB tests (Figure 21) confirm the loss of mechanical strength for PTFE and release agent polluted samples. Moreover, the decrease in wettability (Figure 1 and Figure 2) measured on the polluted adherend surfaces prior to bonding was higher for PTFE pollution than release agent pollution, which is in agreement with the measured critical SERR G_c that is lower for PTFE than for release agent pollution.

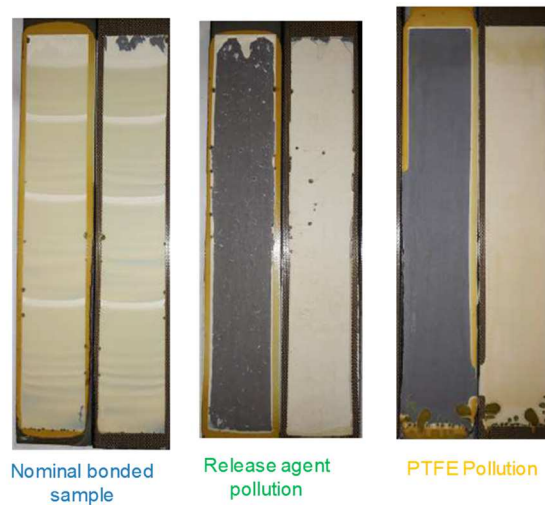


Figure 19: Fracture surfaces of Ti-AF191-Ti bonded samples after DCB tests for different pollutions. (*color should be used in print*)

Nonlinear measurements were performed on ten 1mm-equidistant points in the middle of each sample. The mean amplitude of second harmonic component (expressed in percentage of fundamental component) is shown in Figure 20. Here again, the mean second harmonic level is also higher for PTFE than release agent polluted bonded samples. The degree of nonlinearity thus seems correlated with the degree of bond strength degradation. However, it should be noted here that further investigation should be undertaken for proper correlation between degradation of interface properties with the nonlinear signal amplitude.

Indeed, the two types of pollution introduced here are different in nature so that the mechanisms producing the nonlinear signal could be different.

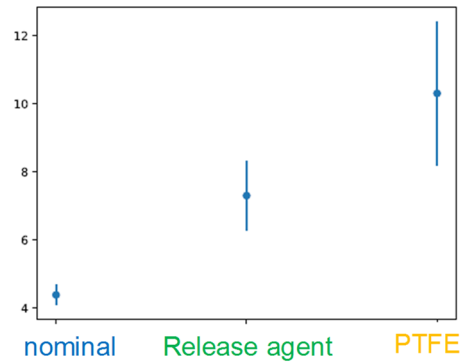


Figure 20: Second harmonic (in percentage of fundamental component) measured on the same bonded Titanium samples as in Figure 19 prior to DCB test (dot: mean of ten 1 mm equidistant points, vertical line: standard deviation). *(color should be used in print)*

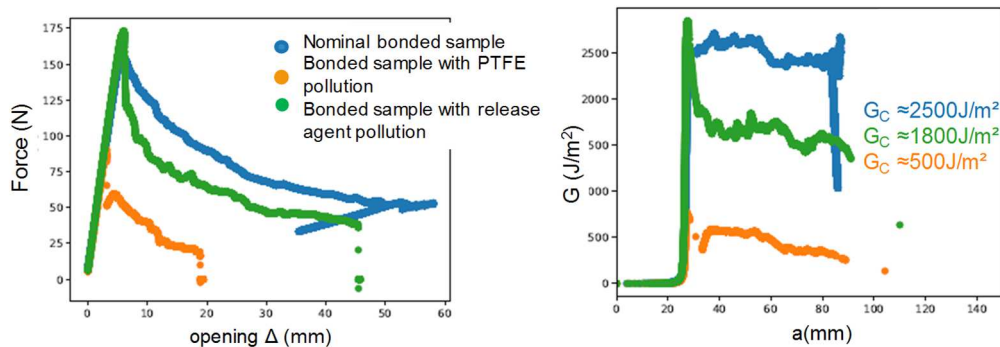


Figure 21: Force-displacement curve (left) measured via DCB test on Titanium bonded samples, either without defect (blue curve) or with uniform pollution (orange curve: PTFE and green curve: release agent); resulting SERR for all cases (right).

(color should be used in print)

5. Conclusions

In this paper, a chaotic cavity transducer is used to detect weak bond in aluminum or Titanium bonded samples. Making use of Time Reversal properties, appropriate long signals are transmitted to classic ultrasonic transducers glued on a highly reverberant piece of Duraluminum (called a time reversal chaotic cavity) so as to focus ultrasound both spatially and in time at desired points on one surface of the cavity. High enough ultrasound amplitudes were reached to perform nonlinear non-destructive testing of adhesion bond. Thin Aluminum and Titanium bonded samples with industrial adhesive were

manufactured. Weak bond was created through controlled surface pollution (PTFE spray, Release agent spray, and fingerprint) after nominal surface preparation prior to bonding, either locally or on the whole surface. Locally high amplitude plane wave was sent to each sample with the chaotic cavity, and second harmonic amplitude measured on the opposite side of the sample using laser interferometer. Destructive DCB tests allowed checking of the type of failure by observing the fracture surfaces and computation of the critical Strain Energy Release Rate. Surface pollution was proved to degrade wettability, and led to adhesive failure and to mechanical strength reduction of the bonded samples. Moreover, harmonic components were measured with the Chaotic Cavity on the polluted regions of the bonded samples. As shown by sessile wetting tests and measured SERR, two different degrees of surface pollution were obtained on Titanium samples using PTFE (high surface degradation) and Release Agent (low surface degradation); the corresponding measured harmonics were shown to increase in the same way (higher amplitude of harmonics for higher surface degradation).

Future work include theoretical analysis to highlight the link between both physical phenomenon (nonlinearity and mechanical strength). Moreover, the correlation of the degradation level of interface properties with the nonlinear signal amplitude should be further investigated using modeling or calibration procedure. Besides, as many industrial components display only one accessible surface, the nonlinear inspection procedure could be adapted to pulse-echo inspection configuration, or even nonlinear Lamb waves inspection. Lastly, the procedure could be applied to composite nonlinear inspection, which is of great industrial interest in the aeronautic field.

Acknowledgements

Raw material for sample preparation was given by Safran.

References

- [1] H. G. Tattersall, «The ultrasonic pulse-echo technique as applied toadhesion testing,» *Journal of Physics D: Applied Physics*, vol. 6, 1973.
- [2] S. I. Rokhlin et M. Rosen, «An ultrasonic method for the evaluation of interface elastic properties,» *Thin Solid Films*, vol. 89, p. 143–148, 3 1982.
- [3] W.-L. Wu, X.-G. Wang, Z.-C. Huang et N.-X. Wu, «Measurements of the weak bonding interfacial stiffness by using air-coupled ultrasound,» *AIP Advances*, vol. 7, p. 125316, 12 2017.
- [4] E. Siryabe, M. Rénier, A. Meziane, J. Galy et M. Castaings, «Apparent anisotropy of adhesive bonds with weak adhesion and non-destructive evaluation of interfacial properties,» *Ultrasonics*, vol. 79, p. 34–51, 8 2017.
- [5] S. I. Rokhlin, «Lamb wave interaction with lap-shear adhesive joints: Theory and experiment,» *The Journal of the Acoustical Society of America*, vol. 89, p. 2758–2765, 6 1991.
- [6] C. Gauthier, M. E.-C. El-Kettani, J. Galy, M. Predoi et D. Leduc, «Structural adhesive bonding characterization using guided Lamb waves and the vertical modes,» *International Journal of Adhesion and Adhesives*, vol. 98, p. 102467, 4 2020.
- [7] B. L. Crom et M. Castaings, «Shear horizontal guided wave modes to infer the shear stiffness of adhesive bond layers,» *The Journal of the Acoustical Society of America*, vol. 127, p. 2220–2230, 4 2010.

- [8] P. Zabbal, «Development of a non-destructive ultrasonic inspection device of a bonded structure using a reverberant cavity with time reversal process,» 2018.
- [9] P. Zabbal, G. Ribay et J. Jumel, «Nondestructive evaluation of adhesive joints by using nonlinear ultrasonics,» *Journal of Physics: Conference Series*, vol. 1184, p. 012003, 3 2019.
- [10] S. Mezil, F. Bruno, S. Raetz, J. Laurent, D. Royer et C. Prada, «Investigation of interfacial stiffnesses of a tri-layer using Zero-Group Velocity Lamb modes,» *The Journal of the Acoustical Society of America*, vol. 138, p. 3202–3209, 11 2015.
- [11] R. Hodé, S. Raetz, J. Blondeau, N. Chigarev, N. Cuvillier, V. Tournat et M. Ducouso, «Nondestructive evaluation of structural adhesive bonding using the attenuation of zero-group-velocity Lamb modes,» *Applied Physics Letters*, vol. 116, p. 104101, 3 2020.
- [12] M. Ducouso, S. Bardy, Y. Rouchasse, T. Bergara, F. Jenson, L. Berthe, L. Videau et N. Cuvillier, «Quantitative evaluation of the mechanical strength of titanium/composite bonding using laser-generated shock waves,» *Applied Physics Letters*, vol. 112, p. 111904, 3 2018.
- [13] B. Ehrhart, B. Valeske et C. Bockenheimer, «Non-destructive evaluation (NDE) of aerospace composites: methods for testing adhesively bonded composites,» chez *Non-Destructive Evaluation (NDE) of Polymer Matrix Composites*, Elsevier, 2013, p. 220–237.
- [14] I. Y. Solodov, N. Krohn et G. Busse, «CAN: an example of nonclassical acoustic nonlinearity in solids,» *Ultrasonics*, vol. 40, p. 621–625, 5 2002.
- [15] D. Yan, B. W. Drinkwater et S. A. Neild, «Measurement of the ultrasonic nonlinearity of kissing bonds in adhesive joints,» *NDT & E International*, vol. 42, p. 459–466, 7 2009.
- [16] C. J. Brotherhood, B. W. Drinkwater et S. Dixon, «The detectability of kissing bonds in adhesive joints using ultrasonic techniques,» *Ultrasonics*, vol. 41, p. 521–529, 9 2003.
- [17] D. Cerniglia, N. Montinaro et V. Nigrelli, «Detection of Disbonds in Multi-layer Structures by Laser-Based Ultrasonic Technique,» *The Journal of Adhesion*, vol. 84, p. 811–829, 12 2008.
- [18] G. Montaldo, D. Palacio, M. Tanter et M. Fink, «Building three-dimensional images using a time-reversal chaotic cavity,» *IEEE Transactions on Ultrasonics, Ferroelectrics and Frequency Control*, vol. 52, p. 1489–1497, 9 2005.
- [19] O. B. Matar, Y. F. Li et K. V. D. Abeele, «On the use of a chaotic cavity transducer in nonlinear elastic imaging,» *Applied Physics Letters*, vol. 95, p. 141913, 10 2009.
- [20] N. Quieffin, «Etude du rayonnement acoustique de structures solides: vers un système d'imagerie haute résolution,» 2004.
- [21] «3MTM Scotch-Weld Structural adhesive film AF 191 Technical Datasheet,» March 2009.
- [22] J. Barkhimer, M. Erich et G. Nair, «Effect of Time Delay Between Etching and Adhesive Bonding (“Outlife” Time) on Lap-Shear Strength of Aluminum Alloys Using Environmentally-Friendly P2 Etch,» 1 Grand Avenue, San Luis Obispo, CA 93407, 2015.
- [23] C. Griffen et D. R. Askins, «Non-chromate surface preparation of aluminum,» University of Dayton Research Institute 300 College Park Avenue Dayton, OH 45469, 1988.
- [24] T. J. Ulrich, A. M. Sutin, T. Claytor, P. Papin, P.-Y. L. Bas et J. A. TenCate, «The time reversed elastic nonlinearity diagnostic applied to evaluation of diffusion bonds,» *Applied Physics Letters*, vol. 93, p. 151914, 10 2008.
- [25] S. Delrue, K. V. D. Abeele et O. B. Matar, «Simulation study of a chaotic cavity transducer based virtual phased array used for focusing in the bulk of a solid material,» *Ultrasonics*, vol. 67, p. 151–159, 4 2016.
- [26] D. Cassereau et M. Fink, «Time-reversal of ultrasonic fields. III. Theory of the closed time-reversal cavity,» *IEEE Transactions on Ultrasonics, Ferroelectrics and Frequency Control*, vol. 39, p. 579–592, 9 1992.
- [27] D. Royer et E. Dieulesaint, *Elastic Waves in Solids I – Free and guided propagation*, Springer, Éd., 2000.
- [28] 3. ISO Norm, *Acoustics-measurement of the reverberation time of rooms with reference to other acoustical parameters*, Geneva, Switzerland: International Organization for Standardization (ISO), 1997.
- [29] D. D. Rife et J. Vanderkooy, «Transfer-Function Measurement with Maximum-Length Sequences,» *J. Audio Eng. Soc.*, vol. 37, p. 419–444, 1989.
- [30] A. Farina, «Simultaneous Measurement of Impulse Response and Distortion with a Swept-Sine Technique,» chez *Audio Engineering Society Convention 108*, 2000.
- [31] G.-B. Stan, J.-J. Embrechts et D. Archambeau, «Comparison of Different Impulse Response Measurement Techniques,» *J. Audio Eng. Soc.*, vol. 50, p. 249–262, 2002.
- [32] D. H. Simpson et P. N. Burns, «Pulse inversion Doppler: a new method for detecting nonlinear echoes from microbubble contrast agents,» chez *1997 IEEE Ultrasonics Symposium Proceedings. An International Symposium (Cat.*

No.97CH36118).

- [33] J. Song, S. Kim, H.-y. Sohn, T.-k. Song et Y. M. Yoo, «Coded excitation for ultrasound tissue harmonic imaging,» *Ultrasonics*, vol. 50, p. 613–619, 5 2010.
- [34] X. Guo, Z.-d. Guan, H.-c. Nie, R.-m. Tan et Z.-s. Li, «Damage tolerance analysis of adhesively bonded composite single lap joints containing a debond flaw,» *The Journal of Adhesion*, vol. 93, p. 216–234, 1 2016.
- [35] A. Melander, J. Linder, H. Stensio, M. Larsson, A. Gustavsson et G. Bjorkman, «How defects in an adhesive layer influence the fatigue strength of bonded steel-sheet specimens,» *Fatigue & Fracture of Engineering Materials and Structures*, vol. 22, p. 421–426, 5 1999.
- [36] B. Blackman et al., «The calculation of adhesive fracture energies from double-cantilever beam test specimens,» *Journal of Materials Science Letters*, 1991.
- [37] E. Moutsompegka, K. Tserpes, M. Noeske, M. Schlag et K. Brune, «Experimental Investigation of the Effect of Pre-Bond Contamination with Fingerprints and Ageing on the Fracture Toughness of Composite Bonded Joints,» *Applied Composite Materials*, vol. 26, p. 1001–1019, 3 2019.
- [38] M. T. Ali, J. Jumel et M. E. R. Shanahan, «Effect of adhesion defects on crack propagation in double cantilever beam test,» *International Journal of Adhesion and Adhesives*, vol. 84, p. 420–430, 8 2018.
- [39] N. B. Salem, M. K. Budzik, J. Jumel, M. E. R. Shanahan et F. Lavelle, «Investigation of the crack front process zone in the Double Cantilever Beam test with backface strain monitoring technique,» *Engineering Fracture Mechanics*, vol. 98, p. 272–283, 1 2013.
- [40] S. Guo, Y. Xia, X. Wei et Q. Zhou, «Investigation on the stable and stick-slip crack propagation behaviors in double cantilever beam test,» *The Journal of Adhesion*, vol. 96, p. 1198–1218, 1 2019.
- [41] F. Tranquart, N. Grenier, V. Eder et L. Pourcelot, «Clinical use of ultrasound tissue harmonic imaging,» *Ultrasound in Medicine & Biology*, vol. 25, p. 889–894, 7 1999.
- [42] T. Petry, R. Knowles et R. Meads, «An analysis of the proposed REACH regulation,» *Regulatory Toxicology and Pharmacology*, vol. 44, p. 24–32, 2 2006.
- [43] M. F. S. F. de Moura, J. J. L. Morais et N. Dourado, «A new data reduction scheme for mode I wood fracture characterization using the double cantilever beam test,» *Engineering Fracture Mechanics*, vol. 75, p. 3852–3865, 9 2008.